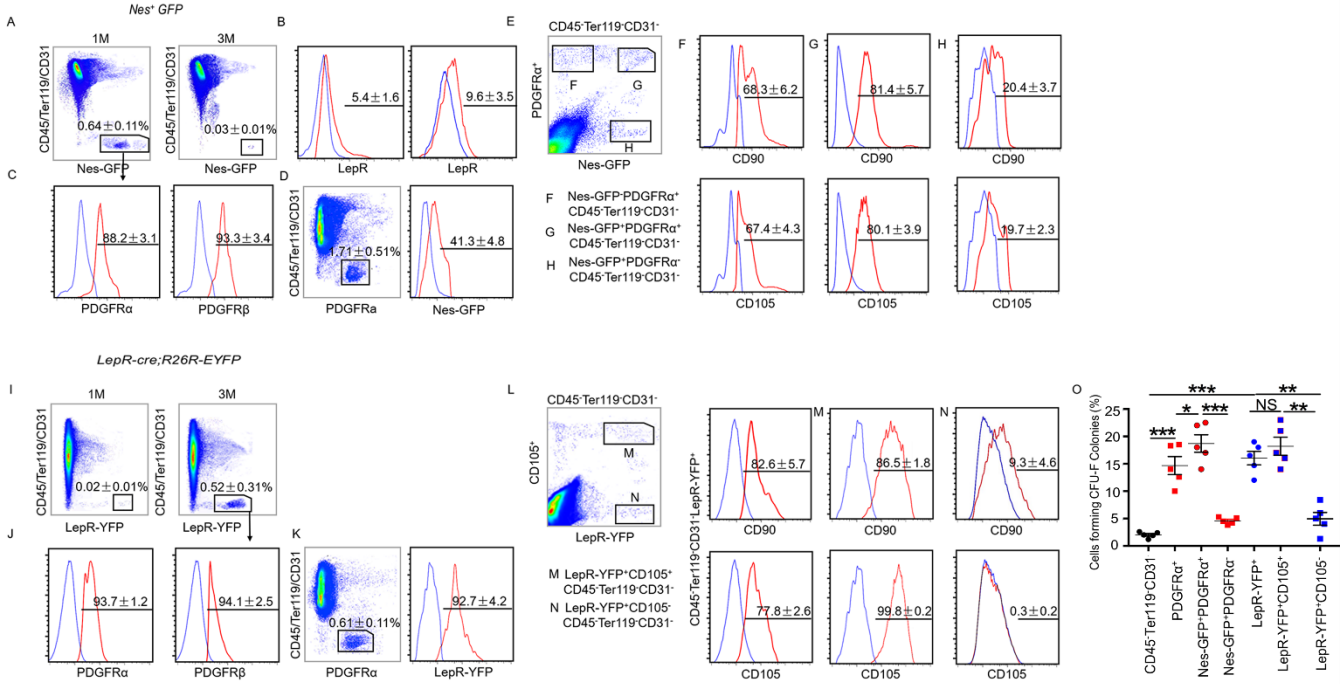

Supplementary Figure 1, related to Figure 2. Subsets of periosteal Nestin$^+$ and LepR$^+$ cells express markers expressed in skeletal stem cells.

(A-H) Flow cytometry analysis of Nestin$^+$ cells in periosteum from *Nestin-GFP* mice. Percentages of Nestin-GFP$^+$CD45$^-$Ter119$^-$CD31$^-$ cells among total periosteum-derived cells (A). Percentage of Nestin-GFP$^+$CD45$^-$Ter119$^-$CD31$^-$ cells that express LepR 1-month-old (B, left panel) and 3-month-old (B, right panel) Nes-GFP mice. Percentage of Nestin-GFP$^+$CD45$^-$Ter119$^-$CD31$^-$ cells that express PDGFRα (C, left panel) or PDGFRβ (C, right panel). PDGFRα$^+$CD45$^-$Ter119$^-$CD31$^-$ cells were FACS sorted from periosteum (D, left panel) (n=5 mice/group). Percentage of the PDGFRα$^+$CD45$^-$Ter119$^-$CD31$^-$ cells that express Nestin-GFP (D, right panel). (E-H) PDGFRα$^+$CD45$^-$Ter119$^-$CD31$^-$ (F), Nestin-GFP$^+$PDGFRα$^+$CD45$^-$Ter119$^-$CD31$^-$ (G), or Nestin-GFP$^+$PDGFRα$^-$CD45$^-$Ter119$^-$CD31$^-$ cells (H) were FACS sorted from periosteum, respectively (E, left panel). Percentage of the cells in (F), (G), and (H) that express CD90 (E, upper right panels) or CD105 (lower right panels) were shown (n=5 mice/group). (I-N) Flow cytometry analysis of LepR$^+$ cells in periosteum from *LepR-cre;R26R-EYFP* mice. Percentages of LepR-YFP$^+$CD45$^-$Ter119$^-$CD31$^-$ among total periosteum- derived cells (I). Percentage of LepR-YFP$^+$CD45$^-$Ter119$^-$CD31$^-$ cells that express PDGFRα (J, left panel) or PDGFRβ (J, right panel). PDGFRα$^+$CD45$^-$Ter119$^-$CD31$^-$ cells were FACS sorted from periosteum (K, left panel) (n=5 mice/group). (L-N) LepR-YFP$^+$CD105$^+$CD45$^-$Ter119$^-$CD31$^-$ (M) or LepR-YFP$^+$CD105$^-$ CD45$^-$Ter119$^-$CD31$^-$ cells (N) were FACS sorted from periosteum, respectively (L, left panel). Percentage of the cells in (M) and (N) that express CD90 (upper right panels) or CD105 (lower right panels) were shown (n=5 mice/group). (O) Percentage of CD45$^-$Ter119$^-$CD31$^-$ periosteal cells expressing each marker that formed CFU-F colonies in culture. ANOVA with Bonferroni post hoc analysis were used to assess statistical significance. Data are presented as mean ± SEM.*$p < 0.05$, **$p < 0.01$, ***$p < 0.001$, N.S. Not Significant.

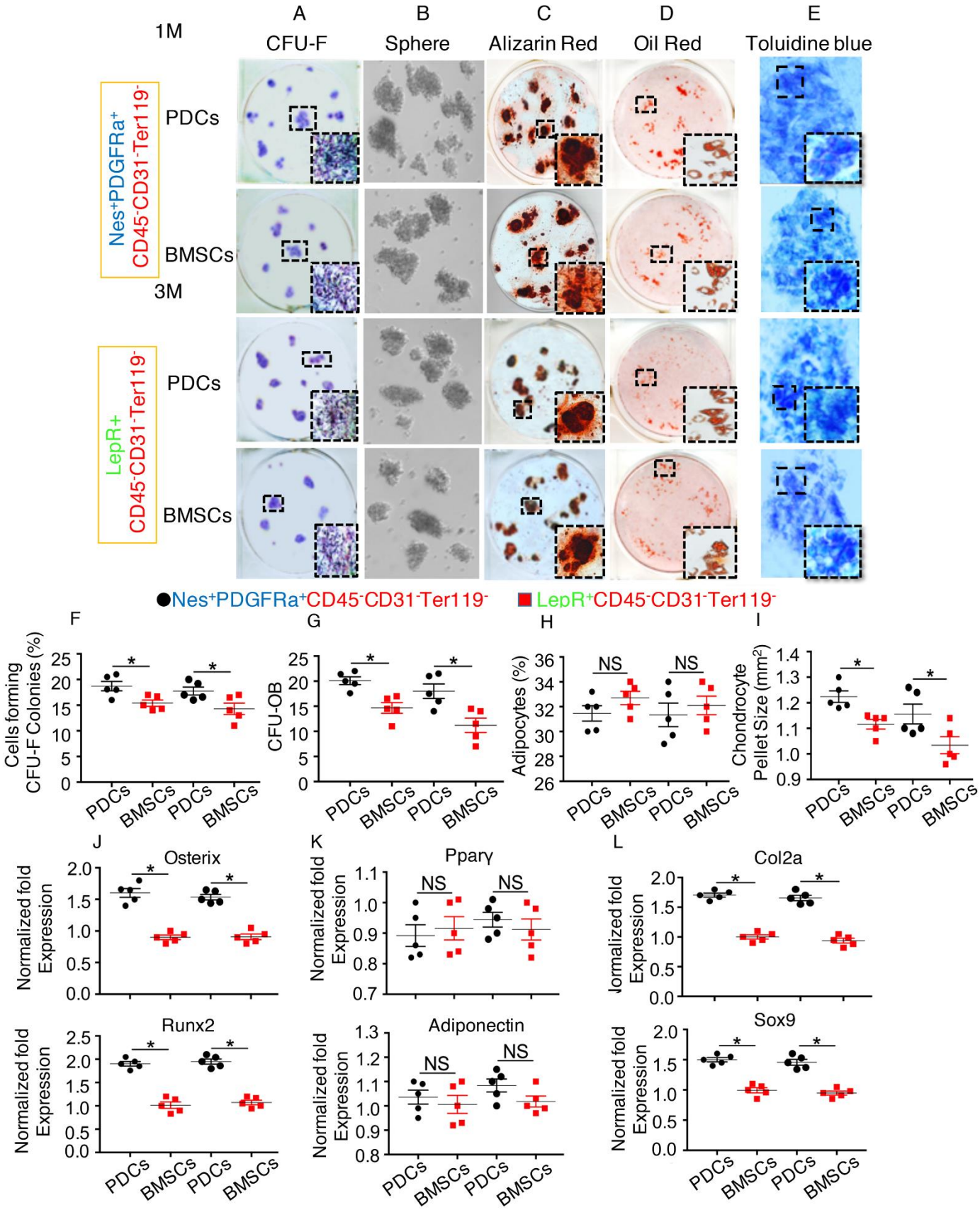

Supplementary Figure 2, related to Figure 2. Periosteal Nestin$^+$ and LepR$^+$ cells form colonies with multi-lineage differentiation capacity. (A-H) Comparison of the biological characteristics of Nestin-GFP$^+$PDGFRα$^+$CD45$^-$ Ter119$^-$CD31$^-$ and LepR-YFP$^+$CD45$^-$Ter119$^-$CD31$^-$ PDCs with bone marrow mesenchymal stromal cells (BMSCs). Colonies (A, F) and spheres (B) formed from sorted Nestin-

GFP$^+$PDGFRα$^+$CD45$^-$Ter119$^-$CD31$^-$ (Upper panels) or LepR-YFP$^+$CD45$^-$Ter119$^-$CD31$^-$ cells (Lower panels) from periosteum or bone marrow as indicated in CFU-F. (n=5 mice/group). Measurement and quantification of colony-derived osteogenic (C, G), adipogenic (D, H), and chondrogenic (E, I) differential ability of Nestin-GFP$^+$PDGFRα$^+$CD45$^-$Ter119$^-$CD31$^-$ and LepR-YFP$^+$CD45$^-$Ter119$^-$CD31$^-$ PDCs and BMSCs by Alizarin Red Staining, Oil Red S Staining, and Toluidine blue staining respectively. Images labeled in the bottom right corner of each figure are higher power with boxes outlining the area. (n=5 mice/group). (J-L) Measure and comparison of Osteogenic (*Osterix*, *Runx2*) (J), Adipogenic (*Pparγ*, *Adiponectin*) (K), and Chondrogenic (*Col2a1*, *Sox9*) (L) differential-related gene expression between Nestin-GFP$^+$PDGFRα$^+$CD45$^-$ Ter119$^-$CD31$^-$ and LepR-YFP$^+$CD45$^-$Ter119$^-$CD31$^-$ PDCs and BMSCs by qRT-PCR. (n=5 mice/group). Two-tailed Student's t tests were used to assess statistical significance. Data are presented as mean ± SEM. *$p < 0.05$. N.S., not Significant.

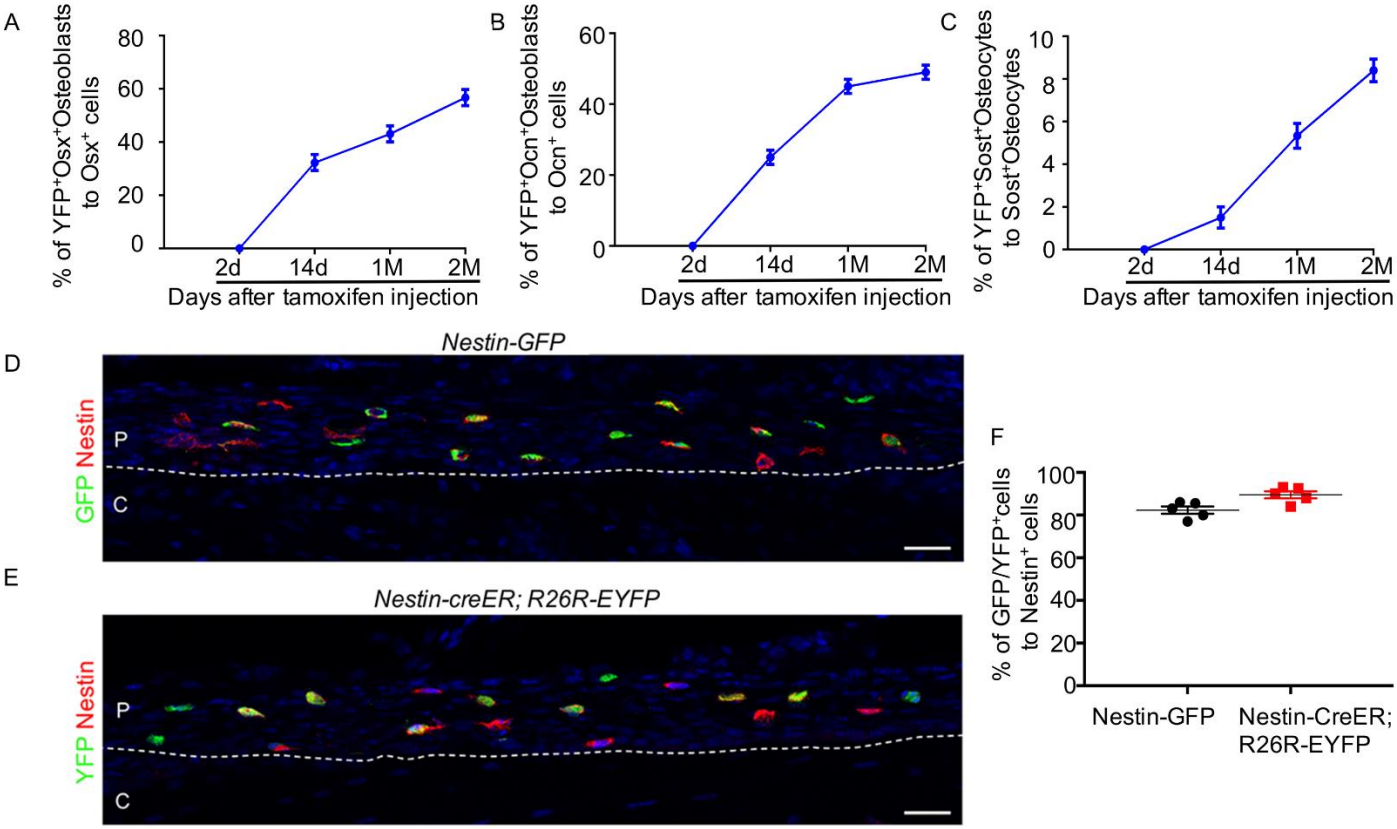

Supplementary Figure 3, related to Figure 2. Periosteal Nestin$^+$ cells contribute to cortical bone growth.

(A-C) Quantification of the percentage of periosteal Osx$^+$ osteoblasts (A), Ocn$^+$ osteoblasts (B), Sost$^+$ osteocytes (C) derived from Nestin$^+$ lineage cells at 2 days, 14 days, 1 month and 2 months following tamoxifen injection in *Nestin-creER;R26R;YFP* mice of 2-week-old. (n=5 mice/group) (D-E) Representative images of tibia diaphyseal periosteum sections from 1-month-old *Nestin-GFP* mice (D) and *Nestin-creER;R26R-EYFP* mice (E, Injected tamoxifen at P28 and chased for 48h) stained for GFP and Nestin. (F) Quantification of the percentage of GFP$^+$ labeled Nestin$^+$ cells to total Nestin $^+$ cells in periosteum. Scale bars, 100 µm. (n=5 mice/group). P, Periosteum. C, Periosteal Cortical bone. Dashed line from (D and E) indicates the limit between periosteum and cortical bone.

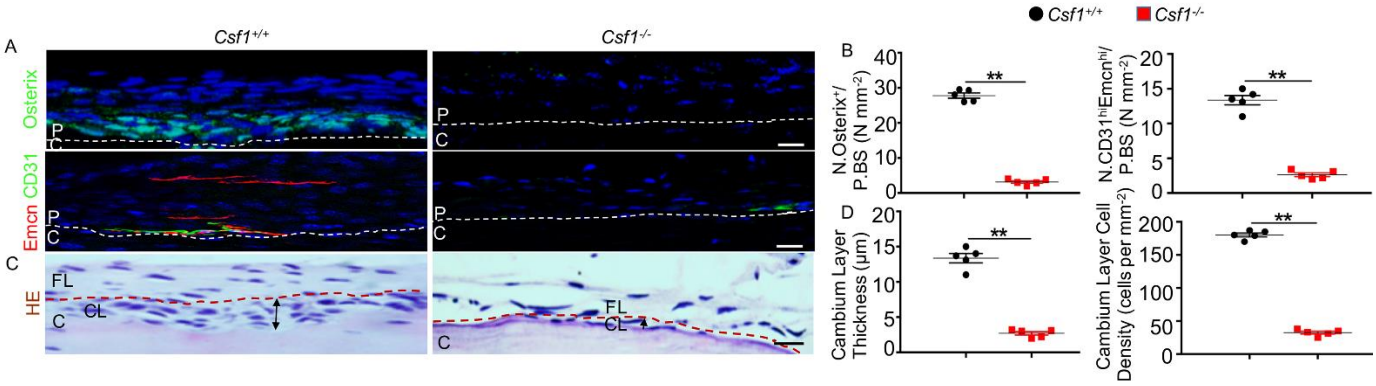

Supplementary Figure 4, related to Figure 3. Macrophage-lineage cell deficiency impairs cortical bone formation and periosteum homeostasis.

(A and B) Representative images of tibia diaphyseal periosteum sections from *CSF1*$^{-/-}$ mice and their control littermates (*CSF1*$^{+/+}$) stained for Osterix (A, top), CD31 and Emcn (A, bottom) and quantification of Osx^{+} osteo-progenitors (B, left panel), and CD31^{hi}Emcn^{hi} vessels (B, right panel) in inner layer adjacent to tibia periosteal surface (N cells/P.BS). Scale bars, 20 µm. (n=5 mice/group). (C and D). H&E staining images of periosteum and quantification of thickness (D, left panel) and cellularity (C, right panel) of inner cambium layer of periosteum. Scale bars, 20 µm. (n=5 mice/group). P, Periosteum. C, Periosteal Cortical bone. BM, Bone Marrow. FL, Fibrous (outer) Layer of periosteum. CL, Cambium (inner) layer of periosteum. Dashed line from (A) indicates the limit between periosteum and cortical bone and from (C) indicates the line between inner layer and outer layer of periosteum. The arrow indicates the width of inner cambium layer. Data are presented as mean ± SEM. *p<0.05, ** p<0.01, N.S., not Significant as determined by Two-tailed Student's t tests.

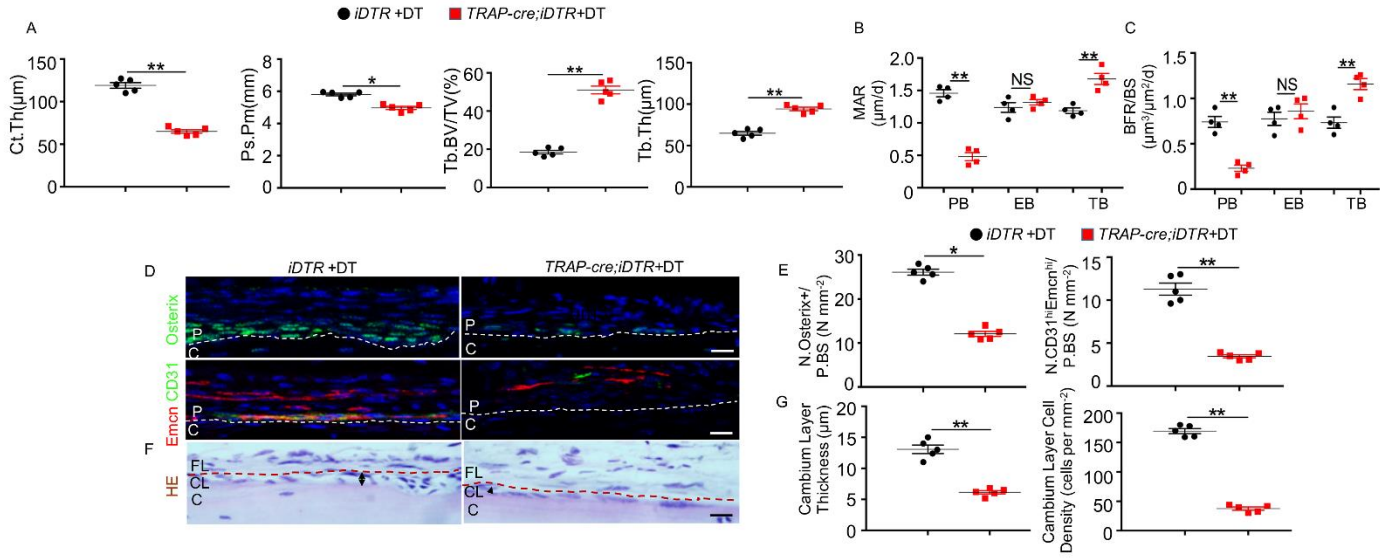

Supplementary Figure 5, related to Figure 4. Ablation of macrophage-lineage TRAP^{+} cells impairs the recruitment of PDCs for cortical bone formation.

(A) Quantitative µCT analysis of periosteal perimeter (Ps. Pm), cortical thickness (Ct. Th), trabecular bone thickness (Tb.Th), and trabecular bone fraction (Tb. BV/TV). (n=5 mice/group). (B and C) Quantification of mineral apposition rate (MAR) and bone formation rate (BFR) of periosteal (PB), endosteal (EB) and trabecular (TB) bone surface from DT-treated *TRAP-cre; iDTR* mice and their control littermates. (n=4 mice/group). (D and E) Representative images of tibia diaphyseal periosteum sections from DT-treated *TRAP-cre; iDTR* mice and their control littermates (DT- treated iDTR mice) for Osterix (D, top), CD31 and Emcn (D, bottom), and quantification of Osx^{+} osteo-progenitors (E, left panel), and CD31^{hi}Emcn^{hi} vessels (E, right panel) in inner layer adjacent to tibia periosteal surface (N cells/P.BS). Scale bars, 20 µm. (n=5 mice /group). (F and G) H&E staining of periosteum (F) and quantitative analysis of thickness (G, left panel) and cellularity (G, right panel) of inner cambium layer of periosteum. Scale bars, 20 µm. (n=5 mice/group). P, Periosteum. C, Periosteal Cortical bone. BM, Bone Marrow. FL, Fibrous (outer) layer of periosteum. CL, Cambium (inner) layer of periosteum. Dashed line from (D) indicates the limit between periosteum and cortical bone and from (F) indicates the limit between inner layer and outer layer of periosteum. The arrow indicates the width of inner cambium layer. Data are presented as mean ± SEM. * $p<0.05$, ** $p<0.01$, N.S., not Significant as determined by Two-tailed Student's t tests.

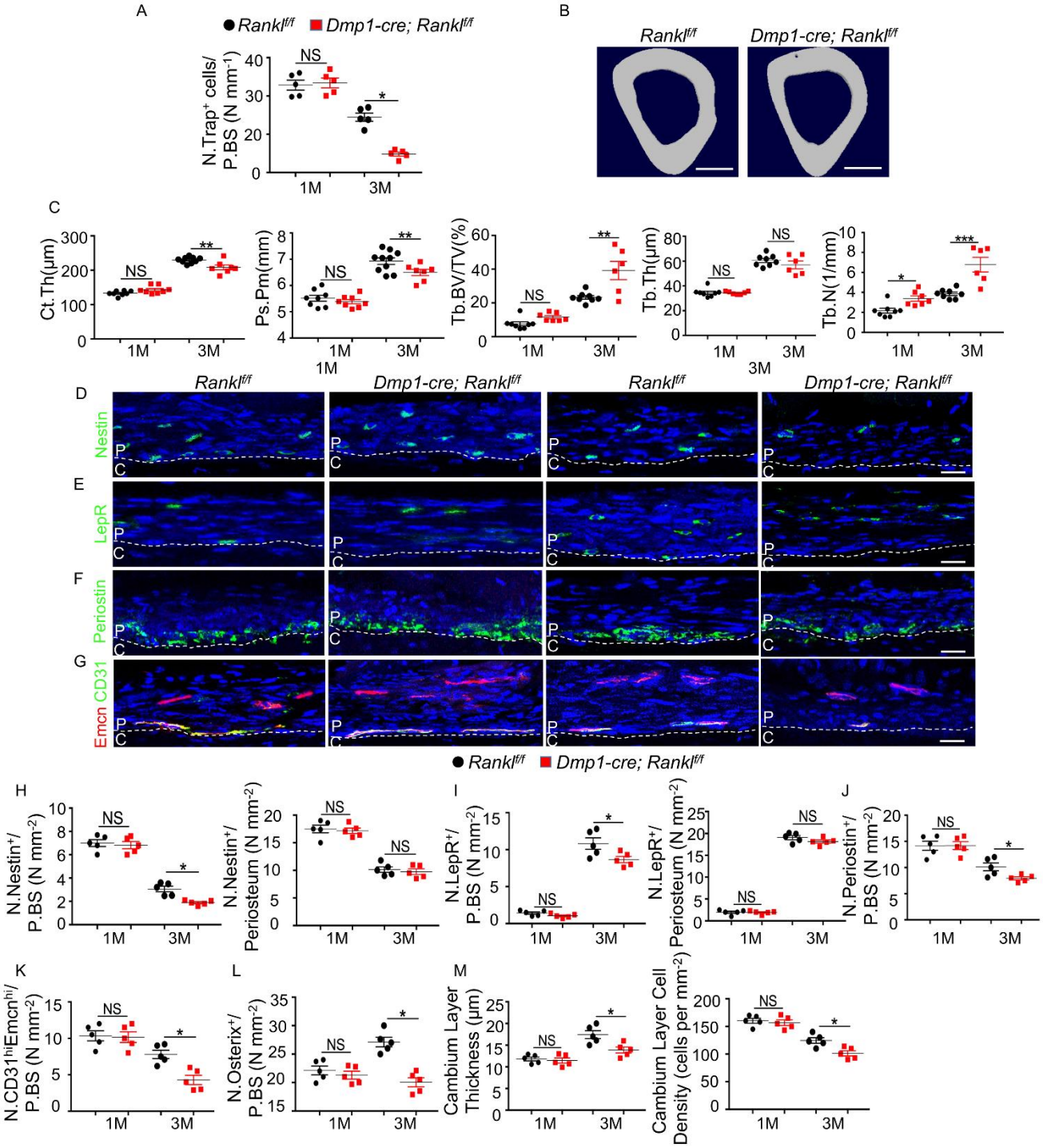

Supplementary Figure 6, related to Figure 4. TRAP$^+$ cell deficiency impairs cortical bone formation.

(A) Quantification of periosteal TRAP$^+$ cells using histochemical TRAP staining from *Dmp1-cre; Rankl$^{f/f}$* mice and their control littermates. (B and C) Representative micro-computed tomography (μCT) images and quantitative μCT analysis of periosteal perimeter (Ps. Pm), cortical thickness (Ct. Th), trabecular bone fraction (Tb. BV/TV), trabecular bone thickness (Tb.Th), and trabecular bone number (Tb.N). 1 M, 1-month-old; 3 M, 3-month-old. (n>6 mice/group). (D-G) Representative images of tibia diaphyseal periosteum from *Dmp1-cre; Rankl$^{f/f}$* mice and their control littermates (*Pdgfb$^{f/f}$* mice) stained for Nestin (D), LepR (E), Periostin (F), CD31 and Emcn (G). (H-L) Quantification of Nestin$^+$ cells (H), and LepR$^+$ cells (I) in inner layer adjacent to tibia periosteal surface (N cells/P.BS) and/or both layers of periosteum (N

cells/Periosteum), and quantification of periostin^{+} cells (J), CD31^{hi}Emcn^{hi} vessels (K) and Osx^{+} osteo-progenitors (L) in inner layer adjacent to tibia periosteal surface (N cells/P.BS). Scale bars, 20 µm. (n=5 mice/group). (M) Quantitative analysis of thickness (M, left panel) and cellularity (M, right panel) of inner layer of periosteum from *Dmp1-cre; Rankl*$^{f/f}$ mice and their control littermates using H&E staining. (n=5 mice/group). P, Periosteum. C, Cortical bone. Dashed line from (D to G) indicates the limit between periosteum and cortical bone. Data are presented as mean ± SEM. * $p<0.05$, ** $p<0.01$, N.S., not Significant as determined by Two-tailed Student's t tests.

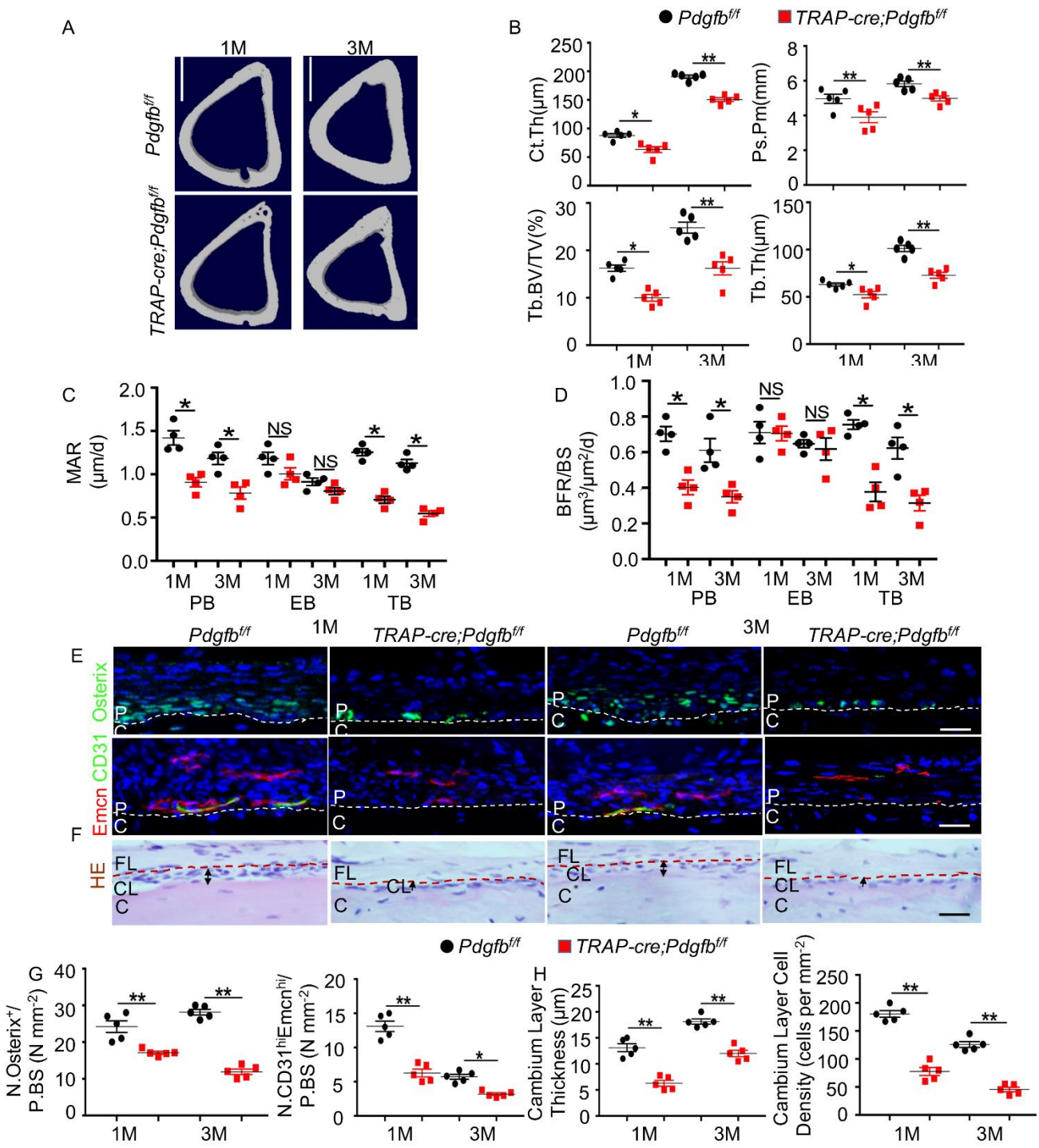

Supplementary Figure 7, related to Figure 5. PDGF-BB secreted by TRAP$^+$ cells modulates periosteal osteogenic microenvironment for periosteal bone formation.

(A and B) Representative micro-computed tomography (μCT) images and quantitative μCT analysis of periosteal perimeter (Ps. Pm), cortical thickness (Ct. Th), trabecular bone thickness (Tb.Th), and trabecular bone fraction (Tb. BV/TV). 1 M, 1-month-old; 3 M, 3-month-old. (n=5 mice/group) (C and D) Quantification of mineral apposition rate (MAR) and bone formation rate (BFR) of periosteal (PB), endosteal (EB) and trabecular (TB) bone surface from *TRAP-cre; Pdgfb$^{f/f}$* mice and their control littermates (*Pdgfb$^{f/f}$* mice). (n=4 mice/group). (E and F) Representative images of tibia diaphyseal periosteum sections from *TRAP-cre; Pdgfb$^{f/f}$* mice and their control littermates (*Pdgfb$^{f/f}$* mice) stained for Osterix (E, top), CD31 and Emcn (E, bottom)

and H&E staining of periosteum(F). (G and H) Quantification of Osx^{+} osteo-progenitors (G, left panel), and $CD31^{hi}Emcn^{hi}$ vessels (G, right panel) in inner layer adjacent to tibia periosteal surface (N cells/P.BS) and quantitative analysis of thickness (H, left panel) and cellularity (H, right panel) of inner cambium layer of periosteum from *TRAP-cre; Pdgfb*$^{f/f}$ mice and their control littermates (*Pdgfb*$^{f/f}$ mice). Scale bars, 20 µm. (n=5 mice/group). P, Periosteum. C, Cortical bone. FL, Fibrous (outer) Layer of periosteum. CL, Cambium (inner) layer of periosteum. Dashed line from (E) indicates the limit between periosteum and cortical bone and from (F) indicates the limit between inner layer and outer layer of periosteum. The arrow indicates the width of inner cambium layer. Data are presented as mean ± SEM. * $p<0.05$, ** $p<0.01$, N.S., not Significant as determined by Two-tailed Student's t tests.

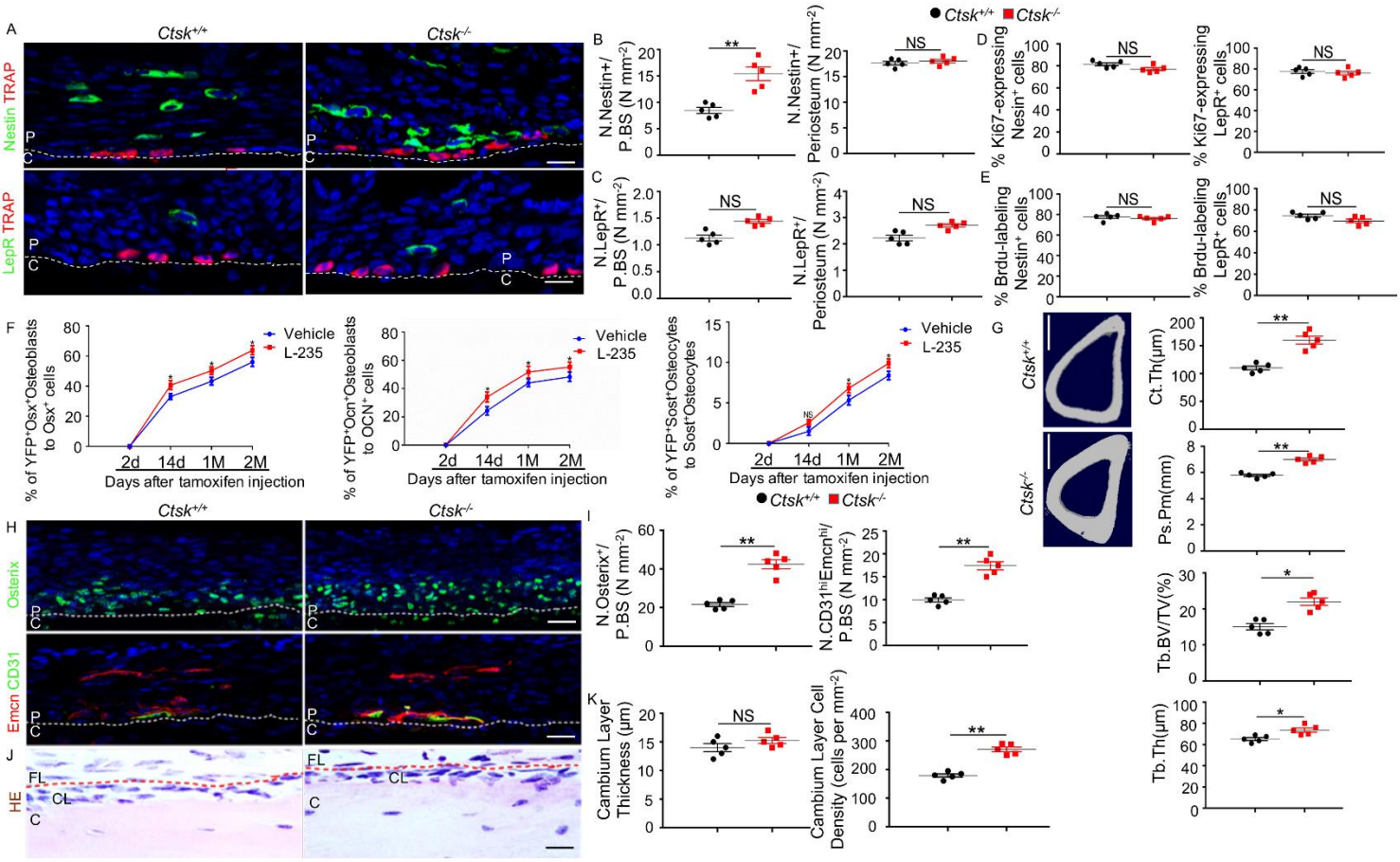

Supplementary Figure 8, related to Figure 5. Increase of PDGF-BB secretion by CTSK inhibitor promotes recruitment of PDCs.

(A-C) Immunofluorescence staining of TRAP and Nestin (A, top), TRAP and LepR (A, bottom) and quantification of Nestin$^+$ cells (B), and LepR$^+$ cells (C) in inner layer adjacent to tibia periosteal surface (N cells/P.BS) and/or both layers of periosteum (N cells/Periosteum) Scale bars, 20 µm. (n=5 mice/group). (D-F) Quantification of Ki67 (D) or Brdu (E) expressing Nestin$^+$ and LepR$^+$ cells in periosteum and the percentage of periosteal Osx$^+$ osteoblasts (F, left panel), Ocn$^+$ osteoblasts (F, middle panel), Sost$^+$ osteocytes (F, right panel) derived from Nestin$^+$ lineage cells (n=5 mice/ group). (G) Representative µCT images and quantitative µCT analysis of periosteal perimeter, cortical thickness, trabecular bone thickness, and trabecular bone fraction. Scale bars, 1mm (n=5 mice/group). (H-K) Immunofluorescence staining of Osterix (H, top), CD31 and Emcn (H, bottom) and quantification of Osx$^+$ osteo-progenitors (I, left panel), and CD31^{hi}Emcn^{hi} vessels (I, right panel) in inner layer adjacent to tibia periosteal surface (N cells/P.BS) and H&E staining of periosteum and quantitative analysis of thickness (K, left panel) and cellularity (K, right panel) of inner layer of periosteum. Scale bars, 20 µm. (n=5 mice/group). P, Periosteum. C, Cortical bone. FL, Fibrous (outer) Layer of periosteum. CL, Cambium (inner) layer of periosteum. Dashed line from (A and H) indicates the line between periosteum and cortical bone and from (J) indicates the line between inner layer and outer layer of periosteum. The arrow indicates the width of inner layer. Data are presented as mean ± SEM. *p<0.05, **p<0.01, N.S., not Significant as determined by Two-tailed Student's t tests.

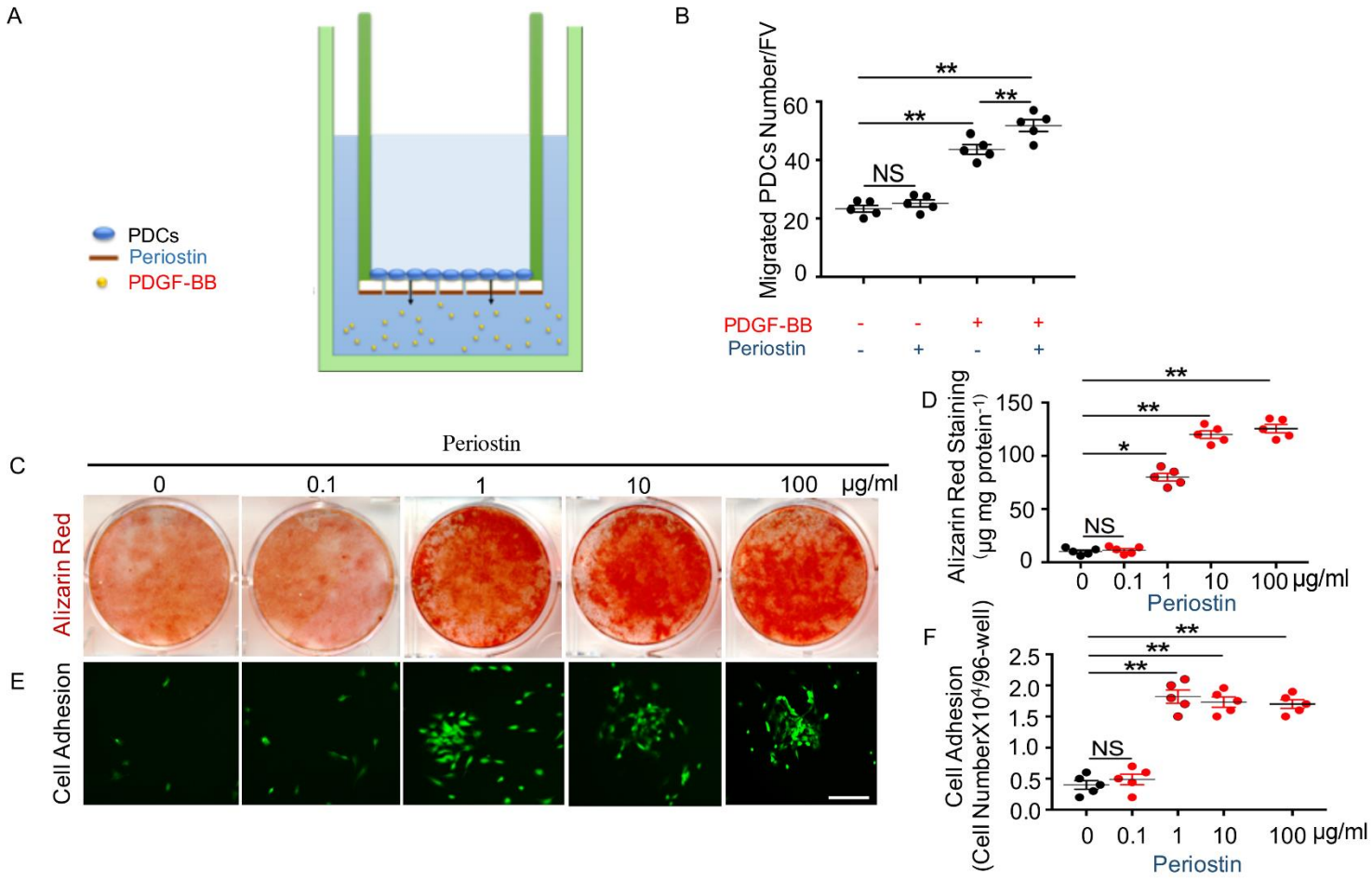

Supplementary Figure 9, related to Figure 6. Periostin promotes osteogenic differentiation and adhesion of PDCs.

(A) Schematic of PDCs-based Trans-well assay. We seeded cells in upper chamber after pre-coated periostin on the lower surface of upper chamber first and added PDGF-BB with culture medium (FBS free) in lower chamber for 4 h. Then the migrated cells were calculated. (B) Numbers of the migrated PDCs at the indicated conditions in the trans-well assays were calculated. (n=5 mice/group). Representative images of Alizarin Red Staining (C) and quantification (D) of osteogenic differentiation of Nestin-GFP^{+}CD45^{-}Ter119^{-}CD31^{-} PDCs treated with different dosages of periostin for 21 days. (n=5 mice/group). (E,F) Measurement (E) and quantification (F) of cell adhesion ability of PDCs with dishes pre-coated with different dosages of periostin for 2 hours. (n=5 mice/group). ANOVA with Bonferroni post hoc analysis was used to assess statistical significance. Data are presented as mean ± SEM. *p<0.05, **p<0.01, N.S. Not Significant.

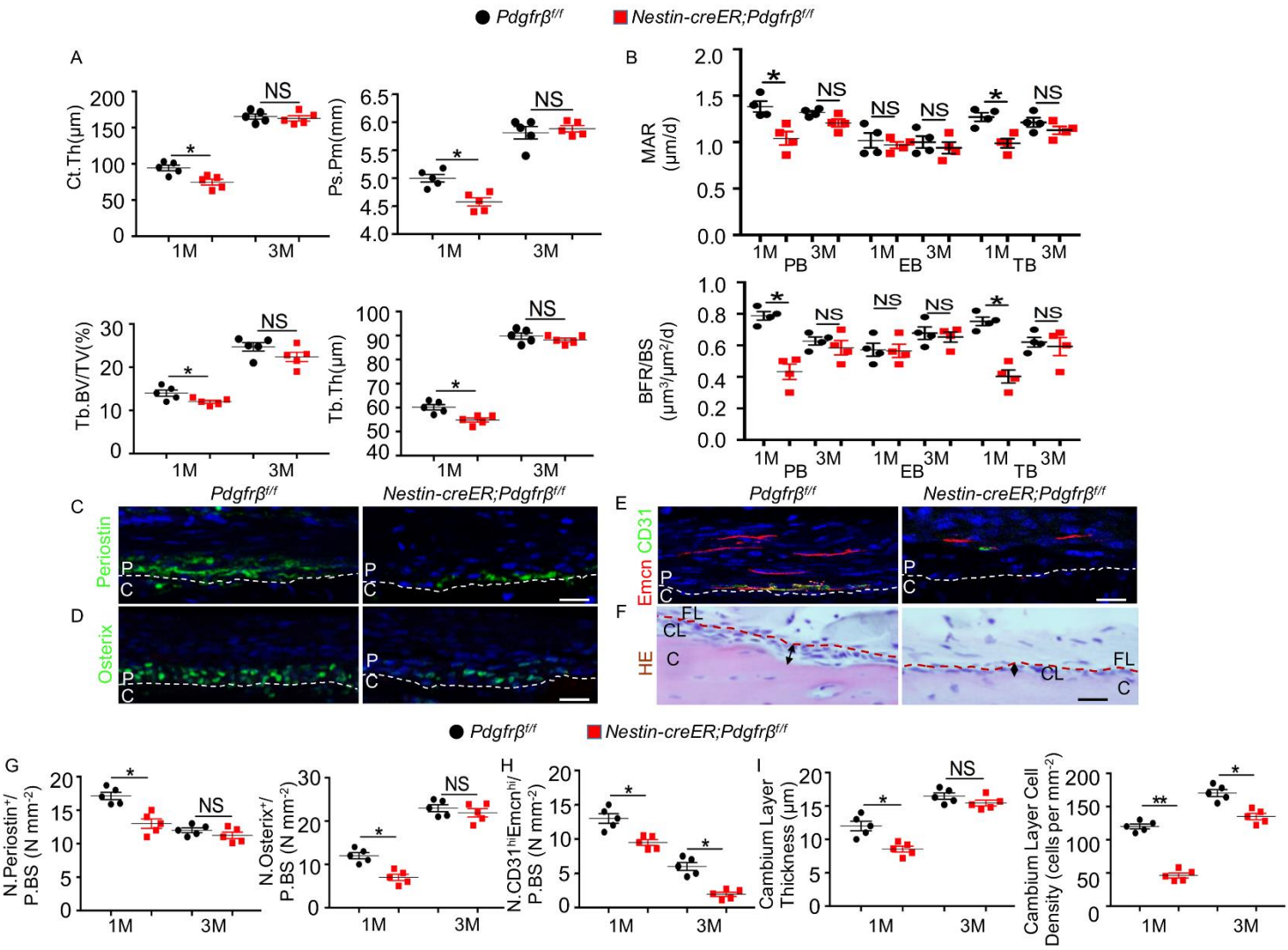

Supplementary Figure 10, related to Figure 7. Deletion of PDGFRβ in Nestin$^+$ cells impairs periosteal osteogenic microenvironment and bone formation.

(A) Representative μCT images and quantitative μCT analysis of periosteal perimeter (Ps. Pm), cortical thickness (Ct. Th), trabecular bone thickness (Tb.Th), and bone fraction (Tb. BV/TV) from *Nestin-creER;Pdgfrβ$^{f/f}$* mice and their control littermates (*Pdgfrβ$^{f/f}$*). 1 M, 1-month-old; 3 M, 3-month-old; Scale bars, 1 mm. (n=5 mice/group). (B) Quantification of mineral apposition rate (MAR) (B, top) and bone formation rate (BFR) (B, bottom) of periosteal (PB), endosteal (EB) and trabecular (TB) bone surface from *Nestin-creER;Pdgfrβ$^{f/f}$* mice and *Pdgfrβ$^{f/f}$* mice. (n=4 mice/group). (C-F) Representative images of tibia diaphyseal periosteum from *Nestin-creER;Pdgfrβ$^{f/f}$* mice and their control littermates (*Pdgfrβ$^{f/f}$* mice) stained for Periostin (C), Osterix (D), CD31 and Emcn (E) and H&E staining of periosteum (F). (G-I) Quantification of Periostin$^+$ cells (G, left panel), Osx$^+$ osteo-progenitors (G, right panel), and CD31^{hi}Emcn^{hi} vessels (H) in inner layer adjacent to tibia periosteal surface (N cells/P.BS) and quantitative analysis of thickness (I, left panel) and cellularity (I, right panel) of inner layer of periosteum from *Nestin-creER;Pdgfrβ$^{f/f}$* mice and their control littermates (*Pdgfrβ$^{f/f}$* mice). Scale bars, 20 μm. (n=5 mice/group). P, Periosteum. C, Cortical bone. FL, Fibrous (outer) Layer of periosteum. CL, Cambium (inner) layer of periosteum. Dashed line from (C-E) indicates the line between periosteum and cortical bone and from (F) indicates the line between inner layer and outer layer of periosteum. The arrow indicates the width of inner layer. Data are presented as mean ± SEM. * $p<0.05$, ** $p<0.01$, N.S., not Significant as determined by Two-tailed Student's t tests.

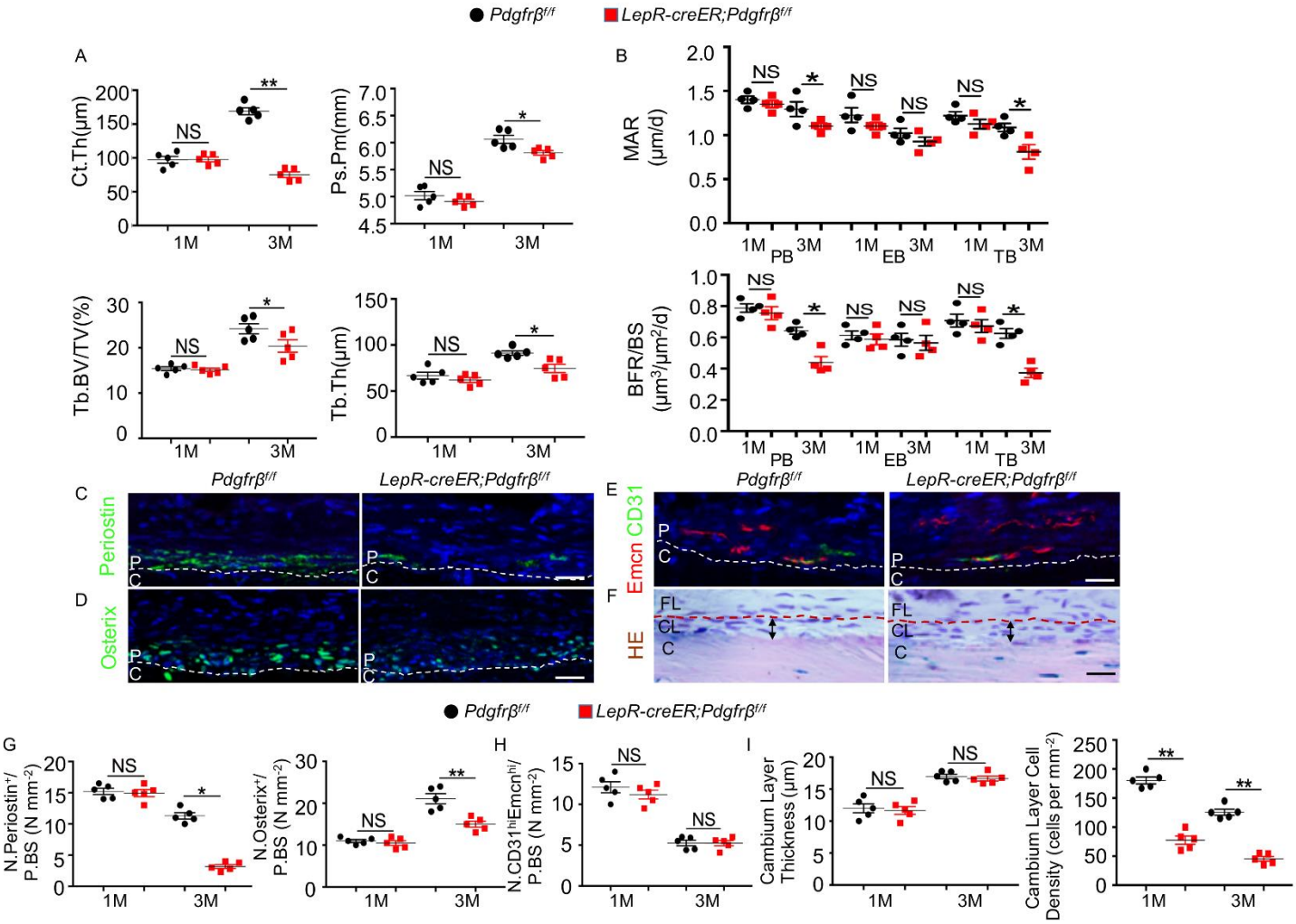

Supplementary Figure 11, related to Figure 8. Deletion of PDGFRβ in LepR$^+$ cells impairs periosteal bone formation.

(A) Representative μCT images and quantitative μCT analysis of periosteal perimeter (Ps. Pm), cortical thickness (Ct. Th), trabecular bone thickness (Tb.Th), and trabecular bone fraction (Tb. BV/TV) from *LepR-cre;Pdgfrβ$^{f/f}$* mice and their control littermates (*Pdgfrβ$^{f/f}$*). 1 M, 1-month-old; 3 M, 3-month-old; Scale bars, 1 mm. (n=5 mice/group). (B) Quantification of mineral apposition rate (MAR) (B, top) and bone formation rate (BFR) (B, bottom) of periosteal (PB), endosteal (EB) and trabecular (TB) bone surface from *LepR-cre; Pdgfrβ$^{f/f}$* mice and their control littermates (*Pdgfrβ$^{f/f}$* mice). (n=4 mice/group). (C-F) Representative images of tibia diaphyseal periosteum from *LepR-cre; Pdgfrβ$^{f/f}$* mice and their control littermates (*Pdgfrβ$^{f/f}$* mice) stained for Periostin (C), Osterix (D), CD31 and Emcn (E) and H&E staining of periosteum (F). (G-I) Quantification of Periostin$^+$ cells (G, left panel), Osx$^+$ osteo-progenitors (G, right panel), and CD31^{hi}Emcn^{hi} vessels (H) in inner layer adjacent to tibia periosteal surface (N cells/P.BS) and quantitative analysis of thickness (I, left panel) and cellularity (I, right panel) of inner layer of periosteum from *LepR-cre; Pdgfrβ$^{f/f}$* mice and their control littermates (*Pdgfrβ$^{f/f}$* mice). Scale bars, 20 μm. (n=5 mice/group). P, Periosteum. C, Cortical bone. FL, Fibrous (outer) Layer of periosteum. CL, Cambium (inner) layer of periosteum. Dashed line from (C-E) indicates the line between periosteum and cortical bone and from (F) indicates the line between inner layer and outer layer of periosteum. The arrow indicates the width of inner cambium layer. Data are presented as mean ± SEM. *p<0.05, **p<0.01, N.S., not Significant as determined by Two-tailed Student's t tests.

A

	Nestin+ PDCs		LepR+ PDCs	
	Puberty	Adult	Puberty	Adult
Cortical bone formation	+	NS	NS	+
Periostin	+	NS	NS	+
Osterix+ osteoblast	+	NS	NS	+
Emcn+CD31+ vessel	+	+	NS	NS
Periosteum (Inner layer) thickness	+	NS	NS	NS
Periosteum (Inner layer) cellularity	+	+	NS	+

B

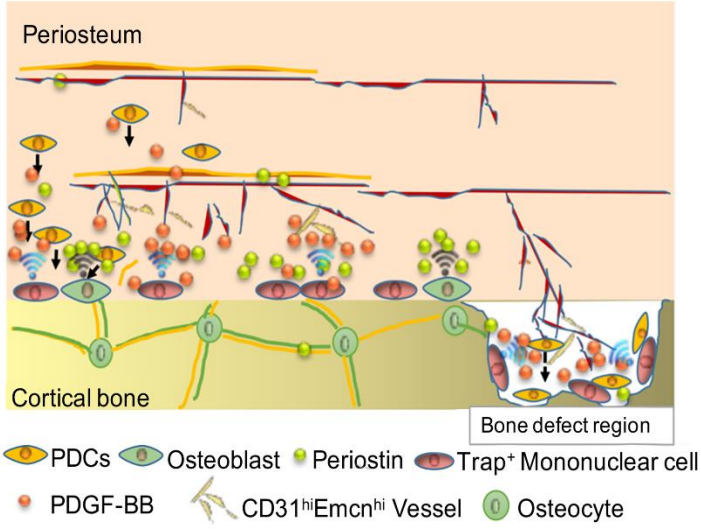

Supplementary Figure 12, related to Figure 7 and 8. Diagram summarizing the mechanism of periosteal TRAP+ mononuclear cells to recruit PDCs during cortical bone formation and regeneration.

(A) Different roles of Nestin+ PDCs and LepR+ PDCs in young and adult mice for periosteal bone formation. + means the condition in which PDCs play roles; N.S. means the condition in which PDCs have no effects. (B) Schematic of the mechanism by which periosteal TRAP+ mononuclear cells regulate the function of PDCs for periosteal bone formation. Periosteal TRAP+ cells in macrophage-lineage regulate cortical bone formation and regeneration in a spatial-temporal manner by producing PDGF-BB, which induces the migration of PDCs from outer layer to periosteal osteogenic bone surface. PDGF-BB secreted by TRAP+ mononuclear cells also provides an essential osteogenic microenvironment coupled with H-type vessel formation in periosteum by transcriptionally inducing the expression of periostin, which supports PDCs adhesion to periosteal bone surface and osteogenic differentiation.

Supplementary Table 1. Primers used for ChIP-PCR

Primers	Forward	Reverse
Frag#1	AAGCACTCTGATTTCTTCATC	GCTCAGAGTGGAACGATTTCA
Frag#2	GACCAAGGGCATCCTGCTTAT	CAGCTACATAATGAACCATTT
Frag#3	GCTATGGAAATATTGTACTGAA	AATTCTTTCAAGCTAACAATCT

Supplementary Table 2. Primers used for quantitative real-time polymerase chain reaction

Primers	**Forward**	**Reverse**
Periostin	TGACTGGAAGAGCGGAGAGTACT	GGTCTGACCTGTCTCCATGTTG
Osterix	ATGGCGTCCTCTCTGCTTGA	GAAGGGTGGGTAGTCATTTG
Runx2	TTACCTACACCCCGCCAGTC	TGCTGGTCTGGAAGGGTCC
Pparg	ACCACTCGCATTCCTTTGAC	TGGGTCAGCTCTTGTGAATG
Adiponectin	TGTTCCTCTTAATCCTGCCCA	CCAACCTGCACAAGTTCCCTT
Col2a1	GTGGAGCAGCAAGAGCAAGGA	CTTGCCCCACTTACCAGTGTG
Sox9	GAACAGACTCACATCTCT	GTGGCAAGTATTGGTCAA
Sca1	TGTGTTACTCAGGAGGCAGCAGTT	TAGGAGGGCAGATGGGTAAGCAAA